Research in Microbiology 174 (2023) 104116

Contents lists available at ScienceDirect

Research in Microbiology

journal homepage: www.elsevier.com/locate/resmic

Original Article

Decoding the chromosome-scale genome of the nutrient-rich *Agaricus subrufescens*: a resource for fungal biology and biotechnology

Carlos Godinho de Abreu [a], Luiz Fernando Wurdig Roesch [b], Fernando Dini Andreote [c], Saura Rodrigues Silva [b], Tatiana Silveira Junqueira de Moraes [a], Diego Cunha Zied [d], Félix Gonçalves de Siqueira [e], Eustáquio Souza Dias [a], Alessandro M. Varani [f, **], Victor Satler Pylro [a, *]

[a] Department of Biology, Federal University of Lavras - UFLA, Lavras, Minas Gerais, Brazil
[b] Department of Microbiology and Cell Science, University of Florida, Gainesville, FL, USA
[c] Department of Soil Science, "Luiz de Queiroz" College of Agriculture, University of São Paulo, Piracicaba, SP, Brazil
[d] Department of Crop Production, School of Agricultural and Technological Sciences, São Paulo State University (UNESP), Dracena, São Paulo, Brazil
[e] Laboratory of Biochemical Processes, EMBRAPA Agroenergia, Brasília, DF, Brazil
[f] UNESP - São Paulo State University, School of Agricultural and Veterinarian Sciences, Department of Agricultural and Environmental Biotechnology, Campus Jaboticabal, CEP 14884-900, SP, Brazil

ARTICLE INFO

Article history:
Received 12 May 2023
Accepted 7 August 2023
Available online 11 August 2023

Keywords:
Agaricus subrufescens
Basidiomycetes
Hybrid DNA sequencing
Chromosome-scale genome assembly

ABSTRACT

Agaricus subrufescens, also known as the "sun mushroom," has significant nutritional and medicinal value. However, its short shelf life due to the browning process results in post-harvest losses unless it's quickly dehydrated. This restricts its availability to consumers in the form of capsules. A genome sequence of *A. subrufescens* may lead to new cultivation alternatives or the application of gene editing strategies to delay the browning process. We assembled a chromosome-scale genome using a hybrid approach combining Illumina and Nanopore sequencing. The genome was assembled into 13 chromosomes and 31 unplaced scaffolds, totaling 44.5 Mb with 96.5% completeness and 47.24% GC content. 14,332 protein-coding genes were identified, with 64.6% of the genome covered by genes and 23.41% transposable elements. The mitogenome was circularized and encoded fourteen typical mitochondrial genes. Four polyphenol oxidase (PPO) genes and the Mating-type locus were identified. Phylogenomic analysis supports the placement of *A. subrufescens* in the Agaricomycetes clade. This is the first available genome sequence of a strain of the "sun mushroom." Results are available through a Genome Browser (https://plantgenomics.ncc.unesp.br/gen.php?id=Asub) and can support further fungal biological and genomic studies.

1. Introduction

Agaricus subrufescens, also known as the "sun mushroom" or "medicinal mushroom", is native to Brazil and referred to as "Almond Portobello" or "Royal Sun Agaricus" worldwide [1–7]. It is low in fat, crude fiber, and ash, but high in protein, total carbohydrates, and available carbohydrates [8]. The mushroom is medicinal, containing high levels of bioactive substances such as ergosterol, β-glucans, agaritin, blazeispirol, proteoglycans, lectin, p-coumaric acid, and sodium pyroglutamate [9]. These bioactive compounds have prophylactic and therapeutic benefits, including antimicrobial and immunomodulatory properties [10,11]. Previous studies have isolated bioactive compounds and validated their medicinal potential [12–17]. Also, *A. subrufescens* is a secondary decomposer fungus, which means it can easily colonize substrates that have previously been subjected to the action of other microorganisms [18]. It exhibits versatility by utilizing agricultural waste materials as substrate due to its enzymatic apparatus capable of breaking down complex compounds such as cellulose, hemicellulose, and lignin into simpler and more assimilable compounds, like monomers [19].

* Corresponding author.
** Corresponding author.
E-mail addresses: amvarani@fcav.unesp.br (A.M. Varani), victor.pylro@ufla.br (V.S. Pylro).

https://doi.org/10.1016/j.resmic.2023.104116
0923-2508/

The genus *Agaricus* accounts for approximately 15% of the production of edible mushrooms globally. However, the actual output of *A. subrufescens* is often neglected [20]. In Brazil, *A. subrufescens* ranks fourth among cultivated mushroom species, along with species such as *Flammulina velutipes*, *Pleurotus djamor*, and *Pleurotus eryngii*. The estimated national production is 900 tons per year, which is 6% of the total [8]. However, *A. subrufescens* is highly perishable, and its production for fresh consumption is limited due to rapid darkening, or browning, during processing and storage. The browning effect limits its commercialization mainly to dried mushrooms and powdered form for medicinal capsules.

Among the factors that directly impact the browning of *A. subrufescens* mushrooms, such as production flow, the number of phenolic compounds, storage temperature, and humidity, the production and activity of polyphenol oxidase (PPO) enzymes (tyrosinase and laccase) are notable [21,22]. The browning process results in a final product that does not meet market standards, primarily due to color and appearance being the main factors in defining the mushroom's value [23].

The comparison of fungal genomes can reveal important information on the production of various bioactive compounds and metabolic pathways [24]. High-quality genome assemblies of several mushroom-producing basidiomycete fungi have been reported in recent studies, including *Schizophyllum commune* [25], *Ganoderma lucidum* [26], *Agaricus bisporus* [18], *Volvariella volvacea* [27], *F. velutipes* [28], *Lentinula edodes* [29], *Sparassis crispa* [30], *Auricularia heimuer* [31], *Hericium erinaceus* [32], *Russula griseocarnosa* [33], *Pleurotus ostreatus* [34] and *Phlebopus portentosus* [35]. *A. bisporus*, a species closely related to *A. subrufescens*, has several genome sequences available on a chromosomal scale, with an average size of 30 Mb and ~11,500 genes distributed across 13 chromosomes [18,36].

We assembled and annotated the chromosome-scale genome of *A. subrufescens* ABL 04/49 and compared it with other related genomes. The lack of a complete genome sequence of *A. subrufescens* has impeded a deeper understanding of mechanisms related to bioactive compound biosynthesis, such as PPOs, hindering further studies based on genome editing. However, genome editing techniques have the potential to overcome oxidation issues in mushrooms, creating opportunities for developing improved strains. The prior knowledge of the complete genome of *A. bisporus* was critical in knocking out one of its six PPO genes, reducing PPO activity by 30% and mitigating the browning process.

2. Material and methods

2.1. Sampling and genomic sequencing of A. subrufescens

2.1.1. Strain and cultivation conditions

The *A. subrufescens* strain ABL 04/49 used in this work was retrieved from the fungal culture collection at CECOG-UNESP in Dracena, São Paulo, and reactivated on BDA medium (200 g of potato, 15 g of agar, and 15 g of glucose). The *A. subrufescens* ABL 04/49 strain was discovered in 2004 in a commercial crop in São José do Rio Preto, São Paulo, Brazil. It has been used experimentally for nearly 20 years. According to Zied et al. [37], this strain produces medium-sized mushrooms with a strong texture and has a reduced time to first harvest (approximately 40 days). It also has an average to high yield and thrives at high production temperatures (around 28 °C). Recently, Vieira Junior et al. [38] highlighted its exceptional agronomic performance and its ability to convert vitamin D into ergosterol in both field and protected environments. The dikaryotic, phase of *A. subrufescens* was cultured at 28 °C for 15 days in Erlenmeyer flasks containing 50 ml of malt broth, under constant agitation at 80 rpm. The mycelium was collected from the liquid medium, filtered using a Whatman absorbent filter paper (14 μm), packaged in aluminum paper, frozen in liquid nitrogen, and stored at −80 °C for further DNA extraction.

2.1.2. DNA extraction and purification

The frozen mycelium was macerated and divided into two 50 mL Falcon tubes, each containing 10 mL of lysis buffer (Tris pH 8.0, 200 mM; EDTA pH 8.0, 50 mM; SDS, 2%; NaCl, 250 mM; proteinase K, 100 μg mL^{-1}).

In one tube, the mixture was agitated for 15 min and then incubated at 65 °C for an additional 15 min. One volume of phenol-chloroform was added to the mixture for deproteinization, and the tubes were gently shaken while keeping the mixture chilled. The tubes were then centrifuged at 6700×*g* for 10 min at 4 °C, and the upper phase was collected. The same procedure was repeated with phenol-chloroform (1:1) and then with chloroform-isoamyl alcohol (24:1). After the final deproteinization step, the supernatant was transferred to microtubes containing one volume of chilled isopropanol. The tubes were stored in a freezer, at −20 °C for 30 min, then centrifuged at 9600×*g* for 30 min at 4 °C. The supernatant was discarded, and the pellet was washed with 70% ethanol. The pellet was then dried in a dry bath at 55 °C, and the DNA was resuspended in 20 μL of TE buffer. The other falcon tube was used for high molecular weight (HMW) DNA extraction using the Quick-DNA HMW MagBead Kit (Zymo Research), following the manufacturer's recommendations.

The purity of the extracted DNAs was evaluated using the Nanodrop Lite (Thermo Fisher Scientific, Waltham, MA, USA), and the quantification was performed using the Qubit 4.0 (Thermo Fisher Scientific, Waltham, MA, USA) and the Qubit dsDNA BR Assay Kit.

2.2. Genome sequencing and assembly

2.2.1. Preparation and sequencing of the Illumina MiSeq library

The DNA sample obtained through the phenol-chloroform protocol was sent for sequencing to NGS - Soluções Genômicas (http://ngsgenomics.com.br/) in Piracicaba, São Paulo, Brazil. The construction of the DNA libraries was performed using the Nextera DNA Flex Kit (Illumina), and the sequencing process followed the manufacturer's recommendations. The libraries were paired-end sequenced (2 × 100 bp) on the Illumina MiSeq platform.

2.2.2. Preparation and sequencing of the GridION™ nanopore library

The high molecular weight (HMW) DNA of *A. subrufescens* strain ABL 04/49 was sequenced on a GridION™ platform at the Federal University of Pampa - UNIPAMPA, in São Gabriel, Rio Grande do Sul, Brazil, as described previously [39]. Briefly, approximately 4 μg of unsheared genomic DNA was treated with the Rapid Sequencing Kit (SQK-RAD004; Oxford Nanopore Technologies, UK). The resulting library was sequenced on the GridION™ platform using a Spot-ON Mk1 flow cell (FLO-MIN 106 R9 version; Oxford Nanopore Technologies, UK) with the R9 Library Loading Bead Kit (EXP-LLB001; Oxford Nanopore Technologies, UK). The raw reads were acquired using the MinKNOW software v3.5.6 in a 72-h experiment, and base calling was performed using the Albacore software v2.0.2.

2.3. A. subrufescens strain ABL 04/49 genome stats

The estimation of genome size, heterozygosity, and repeated content assessment was performed through a kmer-based statistical approach using the jellyfish tool [40] and GenomeScope2 [41].

2.4. Hybrid genome assembly of A. subrufescens strain ABL 04/49

A hybrid genome assembly strategy was employed, combining the Illumina short-reads and the GridION long-reads, using MaSuRCA v 4.0.7 software (Maryland Super- Read Celera Assembler) [42]. Chromosomal assembly was performed through a comparative and manual approach, using genomic data from closely related species with complete genomes at the chromosome-scale available at NCBI: *A. bisporus* strain KMCC00040 (GCA_001682475.1) and *A. bisporus* var. *bisporus* H97 (GCA_000300575.2), as references. The primary and alternate assemblies generated by MaSuRCA were used to process the *A. subrufescens* ABL 04/49 genome assembly at the chromosome scale. The RagTag tool [43] was used for this purpose, with minimap2 [44] and JupiterPlot (https://github.com/JustinChu/JupiterPlot) tools used for alignment and visualization. Additionally, the SAMBA tools and the "close_scaffold_gaps.sh" script from the MaSuRCA package were used for manual validation of chromosome assembly. The markers generated in a previous study, which provided the linkage map of *A. subrufescens* [45], were used to guide and validate the assembly at the chromosome level and identify the mating-type locus. The genome assembly was checked for completeness using the BUSCO program [46] with the agaricales_odb10 database, KAT tools (k-mer spectra) [47], and merqury [48].

2.5. Genome structural annotation: transposable elements and genes

The *de novo* detection of TEs (transposable elements) was performed using the EDTA pipeline [49]. The portion of the genome corresponding to TEs was masked (soft-masked) and subsequently used for the structural annotation step. To identify the genetic evidence, we used public RNAseq data from the JSR3 strain of *A. subrufescens* available on GenBank (BioProject ID PRJNA305463) and referring to different stages of development: mycelium, fruiting body, and primordium (SRAs: SRR11871366, SRR11871367, SRR11871368, SRR6407106, SRR6407107, SRR6407108, SRR6407109, SRR6407110, SRR6407111, SRR6407112). These RNA-seq data were assembled with the Trinity tool [50] using the *de novo* and genome-guided approach. These transcriptome assembly results were used by the PASA program [51] to identify gene models.

Subsequently, gene prediction and annotation were performed using the BRAKER 1 + 2 software [52], with RNAseq data used as evidence for BRAKER 1, and OrthoDB database [53] was used as evidence for BRAKER2, according to the recommendations of the BRAKER tool. The BRAKER 1 + 2 and PASA prediction results were combined with the EVIDENCE MODELER tool (Version 1.1.1) [51], and used in two rounds in the PASA tool [51] to identify isoforms and annotation corrections and generate the final structural annotation. The quality of the genomic annotation was assessed by the BUSCO program using the agaricales_odb10 database [46] and compared with the BUSCO completeness obtained by the genomic assembly.

2.6. Functional annotation

All coding regions and predicted isoforms were functionally annotated using EggNOG-mapper Version 1.0, with the EggNOG Version 5.0 database [54], and BLAST searches against the basidiomycete database from the UniProt database [55]. The results were categorized, and functional annotation of each coding region and isoform, as well as Gene Ontology and KEGG enzyme association, were performed using the software Blast2GO [56] and BlastKOALA [57].

2.7. Annotation of secondary metabolites and active enzymes of CAZymes carbohydrates in A. subrufescens

The annotation of secondary metabolites was performed using the FungiSMASH online platform [58]. Glycosyltransferases (GTs), auxiliary activities (AA) and carbohydrate-binding modules (CBMs) in *A. subrufescens* lineage ABL 49, were annotated through the dbCAN2 platform (http://bcb.unl.edu/dbCAN2/blast.php) [59,60].

2.8. Comparative analysis

We used the JupiterPlot tool (https://github.com/JustinChu/JupiterPlot) for comparative analysis on a macrosyntenic scale among *A. subrufescens and* the species *A. bisporus* KMC00540 and *A. bisporus* var. *bisporus* H97. The MCscan tool (https://github.com/tanghaibao/jcvi/wiki/MCscan - Python-version) was used for comparative analysis on a microsyntenic scale of loci containing genes encoding PPOs and mating-type (MAT). The OrthoVenn2 pipeline [61] was used for identifying gene families and conducting GO enrichment comparative analysis. For comparison, the genomes of *A. bisporus* H97 (GCA_000300575.2), and *Saccharomyces cerevisiae* S288C (baker's yeast) (GCA_000146045.2) were used.

2.9. Phylogenomic analysis of A. subrufescens ABL 04/49

The phylogenomic analysis was conducted using the BUSCO Phylogenomics program (a Python pipeline for constructing species phylogenies using BUSCO proteins) (https://github.com/jamiemcg/BUSCO_phylogenomics) in supermatrix mode, using complete genome assembly data. For this analysis, the genomes of the basidiomycetes *A. bisporus* H39 (GCA_001682475.1), *A. bisporus* var. *bisporus* H97 (GCA_000300575.2), *A. bisporus* ARP23 (GCA_006491665.1), *A. bisporus burnettii* H119p4 (GCA_014872705.1), *V. volvacea* V23 (GCA_000349905.1), *L. edodes* W1-26 (GCA_001700625.1), *F. velutipes* KACC42780 (GCA_000633125.1), *P. ostreatus* PC9 (GCA_014466165.1), *P. portentosus* PP17026 (GCA_020232755.1), *Russula griseocranosa* LJ24 (GCA_004801975.1), *H. erinaceus* CS-4 (GCA_006506795.2), and *A. heimuer* Dai_13782 (GCA_002287115.1) were used, in addition to the assembled genome of *A. subrufescens* strain ABL 04/49. The genome of the yeast *S. cerevisiae* S288C (baker's yeast) (GCA_000146045.2) was used as an outgroup.

2.10. Mitochondrial genome assembly, annotation and comparative analyses

The mitochondrial genome of *A. subrufescens* strain ABL 04/49 was obtained from the assembly results. The annotation was carried out using the MFannot platform (https://github.com/BFL-lab/Mfannot). The introns were determined with RNAweasel (https://github.com/BFL-lab/RNAweasel). The mitochondrial genome of *A. bisporus* H97 (JX271275) [62] was used as reference for comparative analyses. The comparative figures were generated with clinker [63] and Kablammo [64].

2.11. Genome browser and access to genomic data

The assembled genome sequence of *A. subrufescens* ABL 04/49 has been deposited with the NCBI under BioProject PRJNA926637 and accession number JAQOTE000000000. Raw genomic sequencing data were deposited in the SRA bank under accession numbers SRR23198184 (Illumina), and SRR23198183 (ONT). The predicted genes/proteins dataset is freely available for download from Zenodo at https://zenodo.org/record/8199855 (https://doi.org/10.5281/zenodo.8199855). A genome browser utilizing

JBrowse2 [65], which contains our complete set of genomic data, is available at: https://plantgenomics.ncc.unesp.br/gen.php?id=Asub.

3. Results and discussion

Our study resulted in the successful generation of a chromosomally-scaled genome assembly of *Agaricus subrufescens*, commonly referred to as the "sun mushroom," with a high-quality annotation that covers 96.5% of the complete genome assembly. The achievement was made possible by utilizing a hybrid assembly approach that combined Illumina short-reads with Oxford Nanopore long-reads, in addition to leveraging available data from previously sequenced *A. bisporus* H97 genome [18], KMCC00540 (www.ncbi.nlm.nih.gov/nuccore/?term=GCA_001682475.1) and a Genetic Linkage Map of *A. subrufescens* [45], allowing for a better understanding of genomic architecture, gene functions and stimulating general research on this mushroom.

3.1. Sequencing and assembly of the A.subrufescens strain ABL 04/49 genome

The dikaryotic genome of *A. subrufescens* strain ABL 04/49 was sequenced by a hybrid approach. We obtained 11,567,801 short-reads (2 × 100bp) and 4,842,231 long-reads (143 kb, N50: 4.4 kb) from the Illumina and GridION™ sequencing platforms, respectively, corresponding to 13.64 Gb of data.

Based on k-mer analyses, the genome of the *A. subrufescens* strain ABL 04/49 demonstrates a heterozygosity rate of 1.48%, with an estimated size of 42 Mb. Approximately 11 Mb of this genome is related to the repetitive fraction (Fig. 1A). The genomic assembly process recovered a total of 54 scaffolds, with an N50 of 1.5 Mb and L50 of 9 Mb. These scaffolds occupy 42 Mb and have coverage of 324 x (Table 1).

The genome size of Agaricomycetes fungi varies from 20 Mb to approximately 200 Mb, with the number of coding regions ranging from 9501 to 39,074 [66]. The average genome sizes of Ascomycota and Basidiomycota fungi are 36.91 Mb and 46.48 Mb, respectively [67]. Similarly, to other fungi of the order Agaricales, *A. subrufescens* ABL 04/49 has a genome size similar to some fungi of that order, and slightly larger than the strains of *A. bisporus* H97 (30.3 Mb) [18], *A. bisporus* ARP 23 (33.4 Mb) [68], and *A. bisporus* var. burnettii H119P4 (30.7 Mb) [36].

The comparative assembly approach utilizing the complete genomes in the chromosomal scale of *A. bisporus* (strains KMC00540 and H97) combined with the use of the RagTag tool and manual analysis enabled the reconstruction of 13 chromosomes and 31 smaller scaffolds (unplaced, totaling 2.5 Mb, N50 152 Kb), in addition to the mitochondrial genome (Tables 2 and 3). The *A. subrufescens* chromosomes were organized and numbered in ascending order of size. Similarly, *A. bisporus* KMC00540 and *A. bisporus* var. bisporus H97 also have 13 chromosomes. It was observed that most of the chromosomes in *A. subrufescens* maintain high levels of synteny to the chromosomes of *A. bisporus*, suggesting low levels of rearrangement between these genomes.

The *A. subrufescens* genetic linkage map, based on 16 linkage groups (LG) [45], was mapped onto the *A. subrufescens* strain ABL 04/49 chromosome level assembly, revealing that the LGs are generally syntenic to the assembly, but with some slight variations (Table S1). For instance, LG2-LG7, LG10, and LG13-LG15 are syntenic, while LG1, LG8, LG9, LG11, LG12, and LG16 exhibit variations when compared to the *A. subrufescens* ABL 04/49 assembly. Indeed, structural variations and complexities within genomic regions, coupled with individual genetic polymorphisms and potential inaccuracies in marker identification, can all contribute to discrepancies between genetic markers and their mapped positions on the genome assembly. However, in general, these results support the assembly of chromosomes I, II, III, IV, VIII, and IX. The other LGs are too small in centimorgan (cM) units and were not considered for further analyses. Furthermore, using previously determined markers, it was possible to identify the mating-type locus (MAT) located on chromosome I.

The final assembly has a BUSCO completeness of 96.5% (C: 96.5% [S: 92.2%, D: 4.3%], F: 0.4%, M: 3.1%, n: 3870), consensus quality value (QV) of 38.49, an error rate of 0.00014, and k-mer completeness of 81.204. K-mer spectra analyses (Fig. 1B) confirm that the genome has heterozygous characteristics and considerable repetitive content.

After structural annotation, 14,332 genes were identified, and a total of 3918 isoforms, totaling 18,250 coding regions (Tables 2 and 3). The structural annotation obtained a BUSCO completeness of 97.5% (C: 97.5% [S:80.2%, D:17.3%], F:0.6%, M:1.9%, n: 3870).

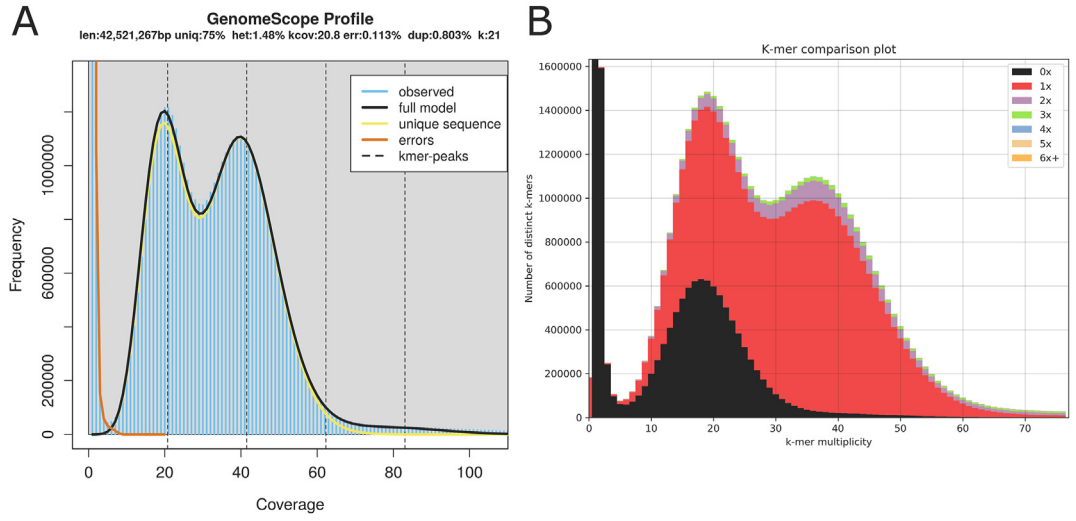

Fig. 1. Analysis of the *A. subrufescens* strain ABL 04/49 genome using the GenomeScope and KAT (k-mer spectra) tools. (A) The GenomeScope analysis reveals a heterozygosity rate of 1.48% in the genome, with an estimated size of 42 Mb. (B) The k-mer spectra analysis confirms the presence of heterozygosity and duplications within the genome.

Table 1
A. subrufescens strain ABL 04/49 genome primary assembly (hybrid assembly) stats.

Parameter	Value
Number of scaffolds	54
Total size of scaffolds	42,004,609 bp
Longest scaffold	4,823,740 bp
Shortest scaffold	21,345 bp
Number of scaffolds > 1k nt	54 (100%)
Number of scaffolds >10k nt	54 (100%)
Number of scaffolds >100k nt	50 (92.6%)
Number of scaffolds > 1M nt	14 (25.9%)
Mean scaffold size	777,863 bp
Median scaffold size	400,172 bp
N50 scaffold length	1,579,673 bp
L50 scaffold count	9

Table 2
General characteristics of the *A. subrufescens* ABL 04/49 genome.

Genome size (bp)	44.531.294
Number of chromosomes	13
Unplaced sequences	31
GC Content (%)	47.24%
Number of genes	14.332
High-quality genes	11.910
tRNAs	185
rRNAs	13
% of genome covered by genes	64.6%
% of the genome covered by TEs	23.41%
% of genome covered by CDS	56.1%
Number of coding sequences (CDS)	18.250
Biggest Gene (bp)	103,448
Biggest CDS (bp)	15,198
Average/exon/gene ratio	7

Approximately 23% (9,793,453 bp) of the genome of *A. subrufescens* ABL 04/49 is composed of transposable elements (TEs) as shown in Table 2. Chromosome VI has the highest concentration of TEs, while chromosomes III and IV have the lowest (Table 3). The majority of these elements belong to the LTR-RT class, with 4.06% as Copy LTR, 5.47% as Gypsy LTR, and 0.06% as unknown LTR. Class II elements make up 2.43% of the *A. subrufescens* ABL 04/49 genome (Tables 3 and 4).

3.2. Functional annotation of A. subrufescens ABL 04/49 genome

Functional annotation of the genome of *A. subrufescens* ABL 04/49 identified 14,332 genes, of which 11,910 (83%) have orthologs in other basidiomycete fungi and were classified as high-quality genes (Table 2). Among these high-quality genes, 6446 were associated with Gene Ontology (GO) terms (Fig. 2), with 4324 annotated by the BlastKoala platform and 3264 having Enzyme Commission numbers (E.C) (Fig. 3A and Fig. S1).

The ability to obtain energy from complex substrates has accompanied these fungi for millions of years through families of conserved genes, mainly the so-called glycoside hydrolases (GHs) [69], and the broad spectrum of GH families necessary to digest cellulose (e.g., GH5, GH6, and GH7) and hemicellulose (e.g., GH3, GH10, and GH43) were found in the genome of *A. subrufescens* ABL 04/49. Three candidate AA2 genes responsible for lignin degradation, as well as 52 genes encoding auxiliary enzymes for lignin degradation, were also found in the genome of *A. subrufescens*. The most abundant classes of enzymes were hydrolases, transferases, and oxidoreductases, while isomerases were the least abundant. A total of 300 CAZymes were identified in the *A. subrufescens* ABL 04/49 genome (Fig. 3B), with 113 containing a signal peptide. The most abundant CAZymes were AA3 (44 occurrences), AA1 (21 occurrences), GH5 (19 occurrences), GH16 and GT2 (11 occurrences), GH18 (10 occurrences), and GH47 (7 occurrences), while the other CAZymes had 1 to 5 occurrences (Table S2).

Peroxidases (PODs) are enzymes that use peroxide as a substrate or oxygen as an electron acceptor to catalyze a large number of oxidative reactions in living organisms [70]. Lignin Peroxidases (LiPs), Manganese peroxidase (MnPs), and versatile peroxidases (VPs) are the main peroxidases for lignin decomposition. The genome of *A. subrufescens* contains three candidate AA2 genes and 52 genes that code for auxiliary enzymes involved in lignin degradation. In contrast, earlier studies have indicated that *A. bisporus* H97 possesses a limited set of peroxidase (POD)

Table 4
Distribution of different classes and lineages of transposable elements in the genome of *A. subrufescens* ABL 04/49.

Class	Count	bp Masked	% Masked
CLASS 01			
LTR (Copies)	1860	1.697.873	4.06
LTR (Gypsy)	1370	2.288.248	5.47
LTR (unknow)	43	25.782	0.06
NonLTR (Line_element)	289	392.125	0.94
CLASS 02			
TIR (CACTA)	482	462.507	1.11
TIR (Mutator)	549	293.688	0.70
TIR (PIF_Hambinger)	43	47.643	0.11
TIR (Tc1_Mariner)	117	122.327	0.29
TIR (hAT)	183	92.201	0.22
NonTIR (helitron)	176	361.215	0.86
Repeat-region	6799	4.009.844	9.59
Total interspersed	11,911	9.793.453	23.41

Table 3
Number and size of chromosomes, genes and transposable elements identified in the *A. subrufescens* ABL 04/49 genome.

Chromosomes	Size (bp)	Number of genes	Count TEs	bp Masked TEs	(%) Masked TEs
I	6,080,401	3227	1482	1,267,774	20.85
II	4,658,285	2651	1297	1,034,171	22.20
III	4,249,451	2420	898	687,619	16.18
IV	3,668,528	2292	606	605,592	16.50
V	3,547,326	1706	1055	875,981	24.69
VI	3,166,853	1297	1722	1,148,347	36.26
VII	3,036,421	1595	731	679,720	22.38
VIII	3,018,530	1534	755	697,196	23.09
IX	2,579,579	1179	998	735,037	28.49
X	2,468,124	1203	829	671,893	27.22
XI	2,308,036	1039	682	694,308	30.08
XII	1,631,491	789	438	333,726	20.45
XIII	1,589,676	760	418	362,089	22.77

machinery for lignin degradation, with only two MnP genes detected in its genome [18].

A. subrufescens genome has 26 gene clusters that encode secondary metabolites. Only four are unique to this fungus, while others are similar to those found in *A. bisporus* H97. Comparative analysis identified six compounds produced, including strobilurin, zaragozic acids, and citrulline (2x). The two citrulline gene clusters in *A. subrufescens* are identical (Table 5).

3.3. Comparative genomics and analysis of polyphenol oxidase (PPO) and mating-type locus (MAT)

A. subrufescens ABL 04/49 exhibits relative macrosynteny among its chromosomes when compared to the genomes of *A. bisporus* KMC00540 and *A. bisporus* var. *bisporus* H97 (Fig. 4 A and B). However, the major differences are located in the telomeric and centromeric regions. The Average Nucleotide Identity (ANI) values

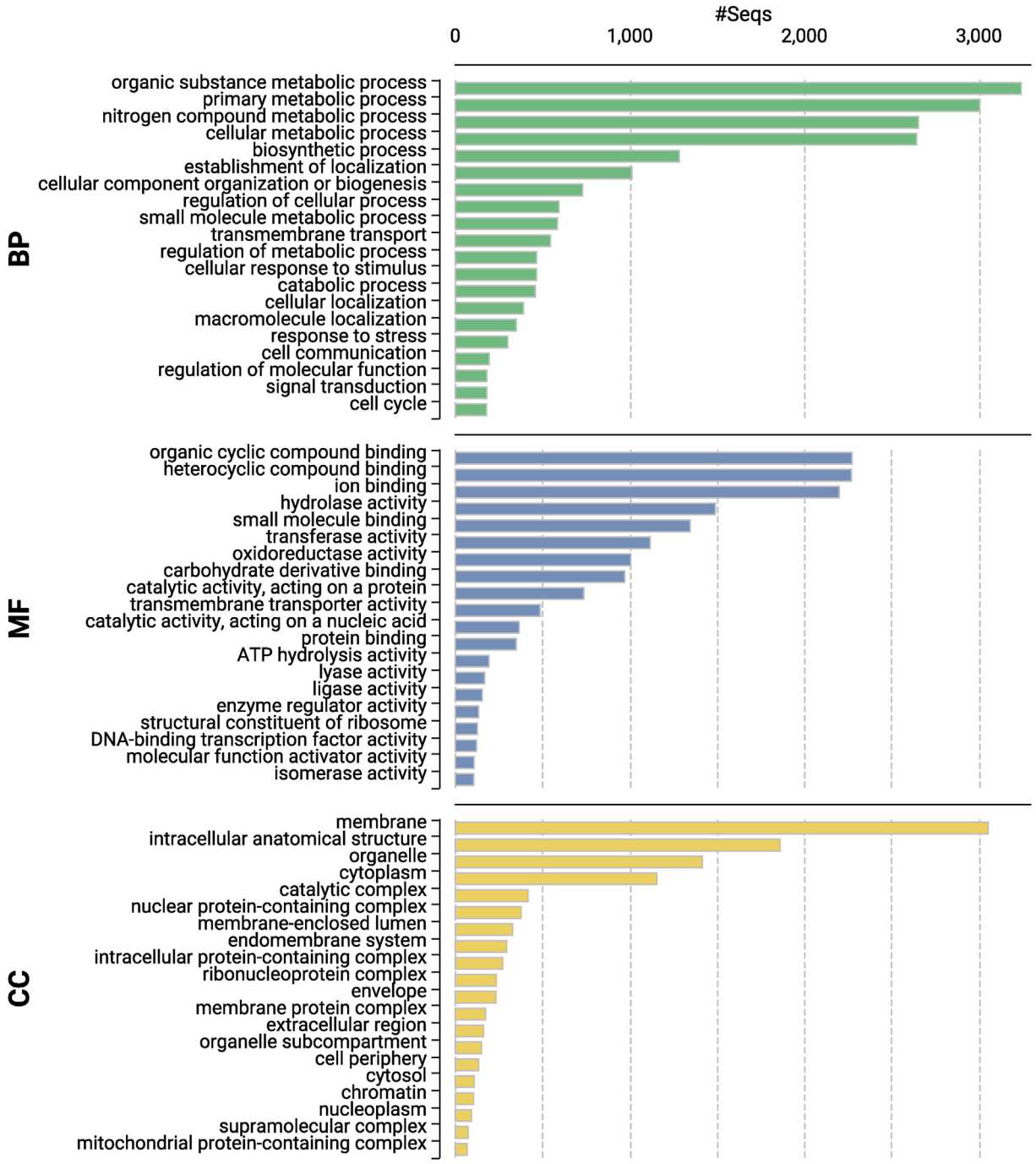

Fig. 2. Gene Ontology (GO) annotation showing the genes with the 20 highest GO counts (GO level 3) for biological processes, cellular components, and molecular functions in *A. subrufescens* ABL 04/49. BP: Biological Process, MF: Molecular Function, CC: Cellular Component.

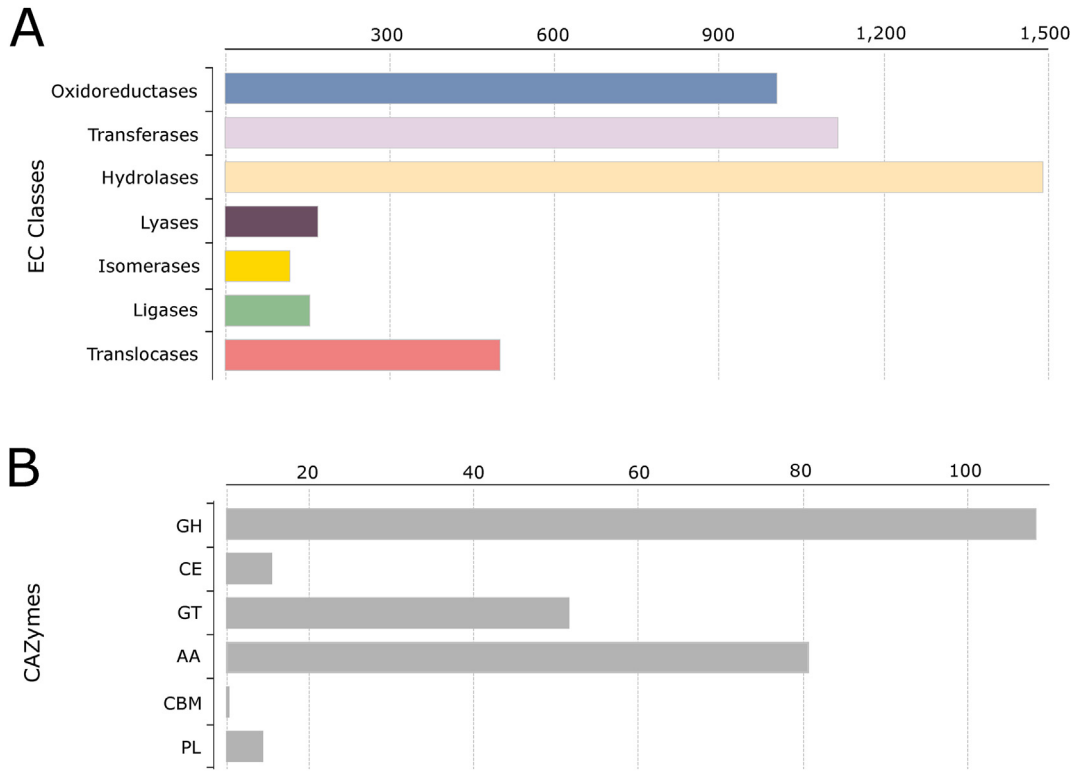

Fig. 3. (A) Distribution of each class of enzymes among genes that have an Enzyme Commission Number (EC number) in the genome of *A. subrufescens* ABL 04/49. (B) Distribution of CAZymes in the genome of *A. subrufescens* ABL 04/49.

between *A. subrufescens* ABL 04/49 and *A. bisporus* species is approximately 77% (SD: 3). Four PPOs were identified in *A. subrufescens* ABL49, mainly distributed on chromosome VII, where three copies are located between positions 2,405,999 and 2,630,868, while the other copy is present on chromosome IX at position 1,129,437 and 1,131,666. Microsynteny analysis, when compared to the genome of *A. bisporus* var. *burnettii* JB137-S8, indicates significant colinearity and synteny among the PPOs present on chromosome VII, but the locus where the PPO is located on chromosome IX exhibits little collinearity (Fig. 4C and D).

In the life cycle of basidiomycetes, the mating type is regulated by two distinct genetic loci [71]. The first locus, typically referred

Table 5
Secondary metabolites identified with the FungiSMASH tool in *A. subrufescens* ABL 04/49.

Location	Loci	Size (nt)	Genes	Type	Probable compound	Comments
chr1	5,627,227..5,648,694	21,468	3	indole	-	100% of genes shared with *A. bisporus* H97
chr2	2,996,287..3,042,352	46,066	25	T1PKS	strobilurin	72% of genes shared with *A. bisporus* H97
chr4	463,223..484,693	21,471	8	trepene	-	-
chr5	1,165,525..1,211,271	45,747	12	NRPS-like	-	46% of genes shared with *A. bisporus* H97
chr5	1,371,559..1,391,756	20,198	11	trepene	Zaragozic acids	70% of genes shared with *A. bisporus* H97
chr5	2,790,670..2,806,197	15,528	6	trepene	citrulline	62% of genes shared with *A. bisporus* H97
chr5	3,329,361..3,350,395	21,035	7	trepene	citrulline	62% of genes shared with *A. bisporus* H97
chr6	206,161..224,020	17,860	9	trepene	-	80% of genes shared with *A. bisporus* H97
chr6	306,613..327,192	20,580	7	trepene	-	-
chr6	367,606..388,871	21,266	8	trepene	-	21% of genes shared with *A. bisporus* H97
chr7	310,444..330,304	19,861	8	trepene	-	100% of genes shared with *A. bisporus* H97
chr7	996,067..1,011,600	15,534	5	siderophore	-	100% of genes shared with *A. bisporus* H97
chr7	1,197,330..1,219,052	21,723	9	trepene	-	100% of genes shared with *A. bisporus* H97
chr8	1,273,004..1,294,151	21,148	13	trepene	-	77% of genes shared with *A. bisporus* H97
chr8	2,892,606..2,936,121	43,516	17	NRPS-like	-	84% of genes shared with *A. bisporus* H97
chr9	1,302,406..1,361,140	58,735	19	NRPS-like T1PKS	strobilurin	88% of genes shared with *A. bisporus* H97
chr9	1,631,217..1,651,794	20,578	7	trepene	-	80% of genes shared with *A. bisporus* H97
chr9	2,122,860 - 2,144,339	21,480	10	trepene	-	75% of genes shared with *A. bisporus* H97
chr10	1,646,832..1,691,126	44,295	15	NRPS-like	-	-
chr11	1,848,916..1,924,880	75,965	26	NRPS-like	-	-
chr12	561,722..598,405	36,684	11	NRPS-like	-	91% of genes shared with *A. bisporus* H97
chr12	1,587,845..1,631,491	43,647	15	NRPS-like	-	50% of genes shared with *A. bisporus* H97
scf7180000000485	18,857..40,004	21,148	13	trepene	-	77% of genes shared with *A. bisporus* H97
scf7180000000485	120,071..178,867	58,797	17	NRPS-like T1PKS	strobilurin	12% of genes shared with *A. bisporus* H97
scf7180000000524	137,619..152,165	14,547	7	trepene	-	60% of genes shared with *A. bisporus* H97
scf7180000000581	39,133..107,365	68,233	20	NRPS-like T1PKS	-	12% of genes shared with *A. bisporus* H97

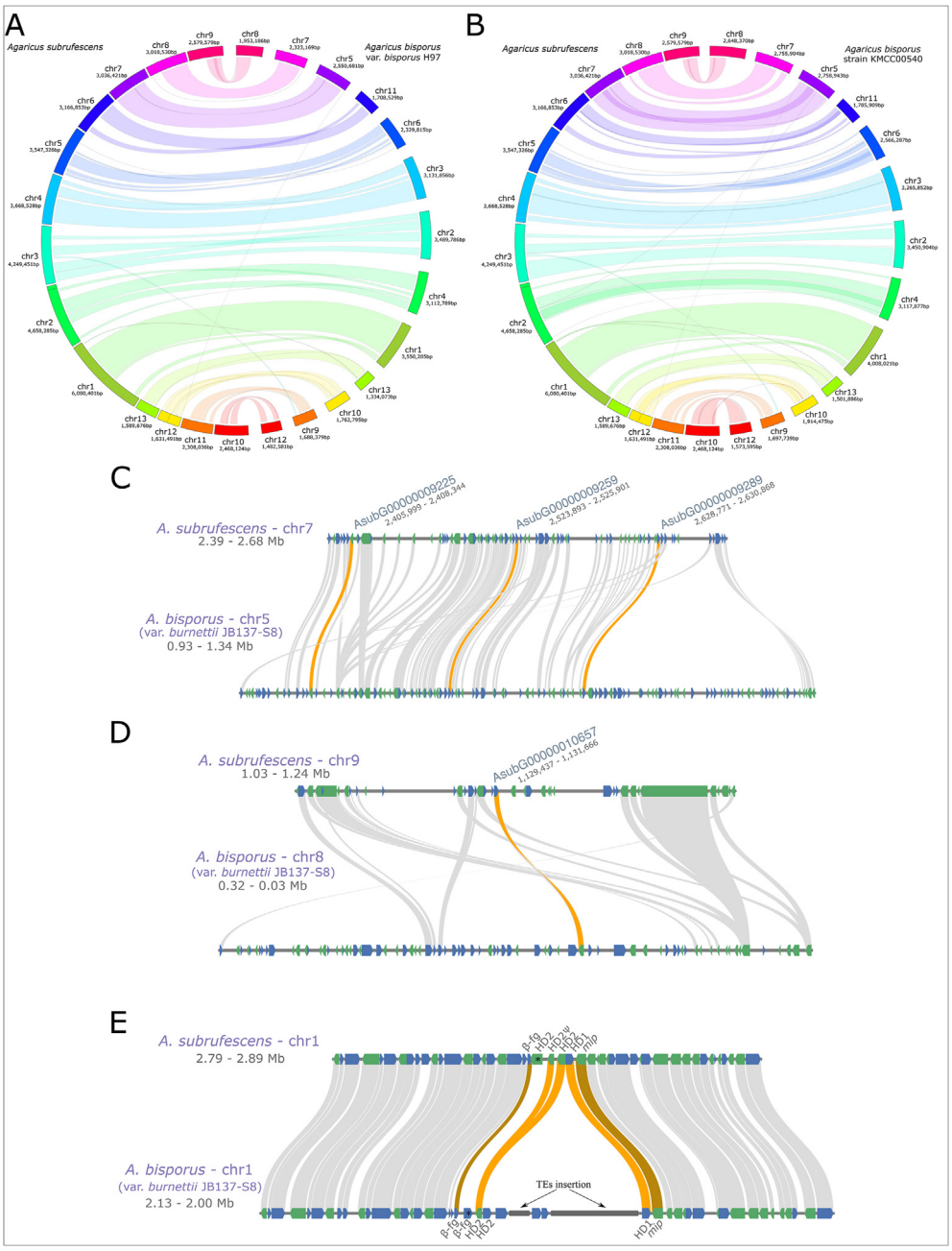

Fig. 4. (A and B) Macrosyntenic scale analysis between chromosomes of *A. bisporus* KMC00540 and *A. bisporus* var. bisporus H97 in comparison to the chromosomes of *A. subrufescens* ABL 04/49. The 13 chromosomes of *A. bisporus* strains are represented by colored blocks on the right, and the 13 chromosomes of *A. subrufescens* strain ABL 04/49 are represented by blocks of the same colors on the left. (C and D) Microsyntenic scale analysis of the Polyphenol oxidase encoding genes locus in *A. subrufescens* ABL 04/49. (E) Mating-type (MAT) locus located on chromosome 1 showing the mip and β-fg genes flanking the homeodomain (HD) transcription factors involved in mating. (For interpretation of the references to color in this figure legend, the reader is referred to the Web version of this article.)

to as the HD or MatA locus, is located on chromosome I. This locus encompasses the mip and β-fg genes, which flank the homeodomain transcription factors (HD) implicated in mating (Fig. 4E). Although both *Agaricus* species share flanking genes collinearity and synteny, the organization of the MatA locus is different between them. For instance, *A. bisporus* var. burnettii JB137-S8 exhibits the insertion of transposable elements between HD1 and HD2 and two copies of the β-fg flanking the HD2 pair, as previously described [71], while *A. subrufescens* ABL 04/49 presents only one β-fg, flanking three HD2 genes. The first *A. subrufescens* ABL 04/49 HD2 gene is exclusive, showing no homologs to *A. bisporus* var. burnettii JB137-S8, and the other two HD2 genes exhibit homologs to *A. bisporus* var. burnettii JB137-S8, but the first *A. subrufescens* ABL 04/49 HD2 copy showing homologs is a pseudogene. Conversely, *A. bisporus* var. burnettii JB137-S8 also exhibits an exclusive HD2 copy. Additionally, the second locus, referred to as the PR or MatB locus, encodes two STE3-type pheromone receptor genes. These genes, which are potentially involved in mating, are located on chromosomes X (1,337,084–1,338,172) and XIII (659,621–661,544). They exhibit homology and synteny with their corresponding loci in the genome of *A. bisporus* var. burnettii JB137-S8.

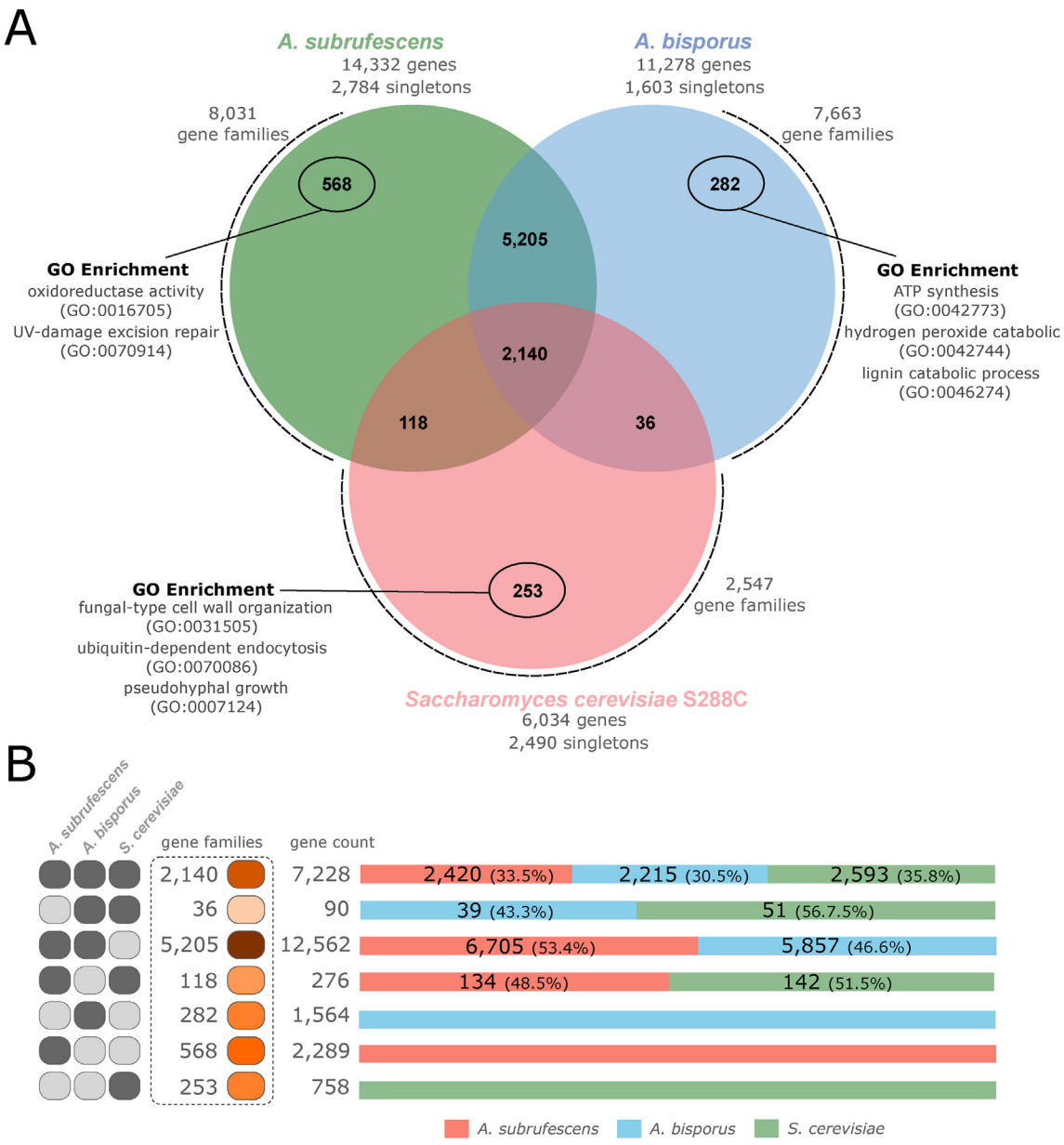

Fig. 5. Gene families shared among *A. bisporus* H97, *Saccharomyces cerevisiae*, and *A. subrufescens* ABL 04/49.

Comparative analysis among *A. subrufescens* ABL49, *A. bisporus* and the yeast *S. cerevisiae* showed that on average, 2300 genes are shared between each species, totaling 2140 gene families (Fig. 5). Enrichment analysis of Gene Ontology (GO) terms for these shared genes determined that biological processes related to rRNA processing (GO:0006364), rRNA methylation (GO:0031167), cytoplasmic translation (GO:0002181), transcription from RNA polymerase II promoter (GO:0006366), proteasome-mediated ubiquitin-dependent protein catabolic process (GO:0043161), and transmembrane transport (GO:0055085) are enriched (p-value <0.05). In contrast, when comparing only within the *Agaricus* genus, 5205 gene families are shared between *A. subrufescens* and *A. bisporus*. The shared genes between these two species of *Agaricus* are enriched for biological processes such as modulation by symbiont of host process (GO:0044003), carbohydrate metabolic process (GO:0005975), cellulose catabolic process (GO:0030245), rRNA processing (GO:0006364), polysaccharide catabolic process (GO:0000272), mRNA cis splicing, via spliceosome (GO:0045292), and xylan catabolic process (GO:0045493). Additionally, molecular functions such as oxidoreductase activity, acting on paired donors, with incorporation or reduction of molecular oxygen (GO:0016705), oxidoreductase activity (GO:0016491), zinc ion binding (GO:0008270), and hydrolase activity (GO:0016787) are enriched (p-value <0.05). Finally, a total of 2289 (568 families), 1564 (282 families), and 758 (253 families) genes were identified as unique to *A. subrufescens* ABL49, *A. bisporus*, and the yeast *S. cerevisiae*, respectively. These unique genes show GO term enrichment (p-value <0.05) specific to each fungus, indicating the genomic particularities of each species (Fig. 5).

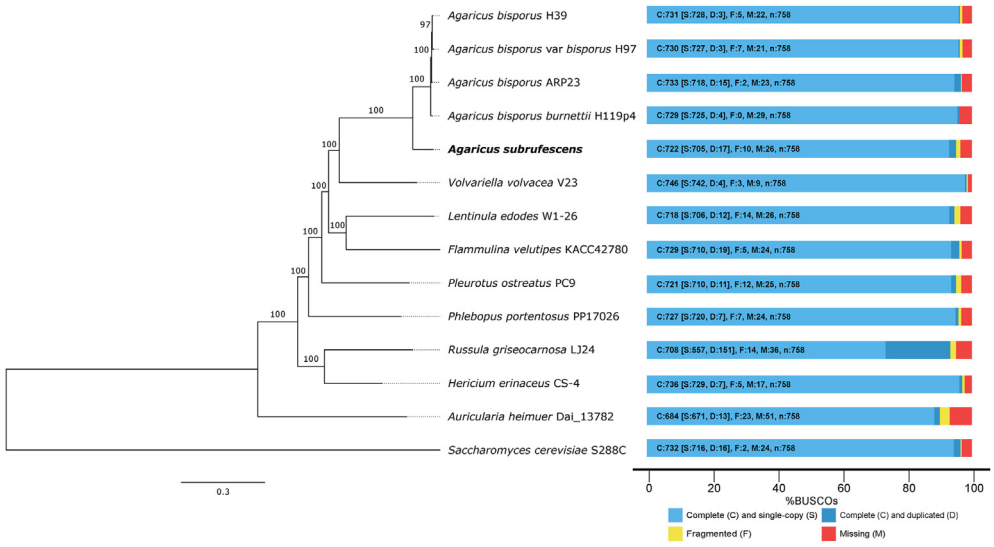

Fig. 6. Phylogenomic tree based on the complete genomes of various edible basidiomycete mushrooms, highlighting the phylogenetic position of *A. subrufescens* ABL 04/49 relative to others and % BUSCO values.

Table 6
Mitochondrial genes identified in *A. subrufescens* ABL 04/49 mitogenome and comparisons against *A. bisporus* H97 [62].

	A. bisporus			*A. subrufescens*		
	Introns	Intron Type	Endonuclease	introns	Type	Endonuclease
nad1	2	2x IB	-	3	3x IB	1x GIY-YIG
nad2	1	IC2	-	0	-	-
nad3	0	-	-	0	-	-
nad4	1	IB	1x LAGLIDADG	1	IB	1x LAGLIDADG
nad4L	0	-	-	0	-	-
nad5	4	2x IB, ID, and II	1x LAGLIDADG	2	2x IB	1x LAGLIDADG and 1x GIY-YIG
nad6	0	-	-	0	-	-
cob	6	5x IB and 1 ID	4x LAGLIDADG	7	4x IB, 2x ID and IA	4x LAGLIDADG
cox1	19	10x IB, ID, IA, 2x IB(3′), IB(5′), and II	11x LAGLIDADG, 5x GIY-YIG, 1x RT	19	13x IB, IA, ID, and 4x IB(5′)	12x LAGLIDADG, 6x GIY-YIG
cox2	2	IC1	2x GIY-YIG	3	3x IB	1x LAGLIDADG, 1 GIY-YIG
cox3	1	IB	1x LAGLIDADG	1	IB	1x LAGLIDADG
atp6	0	-	-	0	-	-
atp8	0	-	-	0	-	-
atp9	0	-	-	0	-	-
rns	0	-	-	1	IC2	1x LAGLIDADG
rnL	5	IA, IB, IC2, and II	1x LAGLIDADG	5	2x IB, 2x IA, and IC2	1x LAGLIDADG

3.4. Phylogenomic analyses

The phylogenomic analyses conducted in this study accurately placed *A. subrufescens* ABL 04/49 within the Agaricomycetes clade, as anticipated. Notably, the sun mushroom (*A. subrufescens* ABL 04/49) formed a distinct clade, separate from the *A. bisporus* lineages (Fig. 6). These findings align with previous investigations into the phylogenetic relationships among *A. bisporus* lineages. In particular, our phylogeny revealed that all four *A. bisporus* lineages examined in this study were grouped together in a monophyletic clade, consistent with the results of O'CONNOR [68].

3.5. Mitochondrial genome and comparative analyses

During the whole-genome sequence assembly process, the complete and circular sequence containing 131,364 bp (27.81% of CG content) of *A. subrufescens* ABL 04/49 mtDNA was successfully obtained as a single scaffold. A total of fourteen typical mitochondrial genes encoding subunits of the electron transport chain and of the ATP-synthase complex (*nad1*, *2*, *3*, *4*, *4L*, *5* and *6*, *cob*, *cox1*, *2* and *3*, *ap6*, *8* and *9*), along with 27 tRNAs and single copies of *rnS* and *rnL*, were identified (Table 6). Most fungal genomes contain a conserved ribosomal protein S3 gene (rps3) for transcriptional regulation and 14 conserved protein-coding genes (nad1, nad2, nad3, nad4, nad4L, nad5, nad6, cob, cox1, cox2, cox3, atp6, atp8, and atp9) that encode subunits of the respiratory chain complexes for energy metabolism [72,73]. In *A. bisporus* H97, 14 genes encoding typical mitochondrial genes that encode subunits of the electron transport chain and ATP synthase complex were observed [62].

We observed significant synteny between the *A. subrufescens* mitochondrial genome and that of the closely-related species *A. bisporus*, highlighting the conservation of genetic organization between these taxa (Fig. 7A). Both mitogenomes exhibit an average nucleotide identity of 86%, with 60% of their mitogenomes sequence being shared (Fig. 7A and B). These similarities also extend to the eroded copies of *rpo1* and *dpo2*, which are shared between both mitogenomes. This observation suggests that the pseudogenization of these genes may represent ancient events that occurred prior to the differentiation of the two species, highlighting

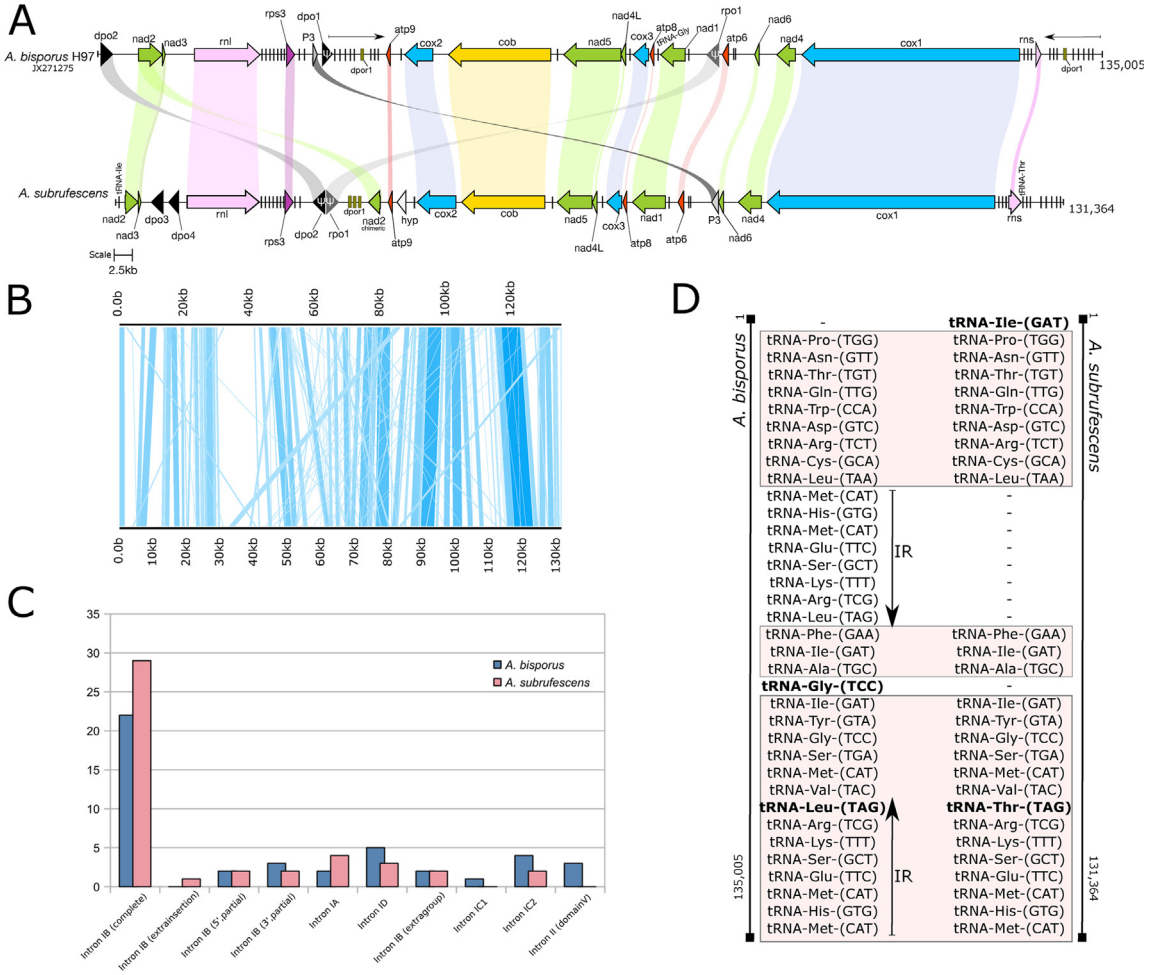

Fig. 7. (A) Schematic representation illustrating the comparisons between *A. subrufescens* and *A. bisporus* mitogenomes. Plasmid-derived and hypothetical sequences are depicted as gray, black, and white arrows, while mitochondrial genes are represented as colored arrows. tRNAs are displayed as small bars. Variations in the tRNA loci are highlighted. The two large inverted repeats in *A. bisporus* are shown as smaller black arrows. (B) Linear representation of discontinuous mega BLAST comparisons between both mtDNA sequences. (C) Bar plot showing the introns types identified in *A. subrufescens* and *A. bisporus* mitogenomes. (D) Positional tRNA comparisons between the two Agaricus mitogenomes.

a shared evolutionary history. In general, these findings demonstrate that the synteny pattern observed in the mitogenomes mirrors the synteny pattern detected between the chromosomes of both species, further emphasizing the conservation of genetic organization across these taxa.

As observed for *A. bisporus* mtDNA [62], the *A. subrufescens* mitochondrial genome also serves as a remarkable reservoir of group I introns (45 group I introns), yet no group II introns were detected (Table 6). Interestingly, the primary differences between both mitogenomes are associated with the number of introns within each gene (Fig. 7C) and the presence of plasmid-derived sequences (Fig. 7A). For instance, while *A. bisporus* mtDNA contains two large inverted repeats that duplicate a cluster of tRNA genes [62] (Fig. 7A and D), *A. subrufescens* mtDNA features two different family B DNA polymerase genes (*dpo3* and *dpo4*). These genes are similar to proteins encoded by DNA *polB* genes described as plasmid-like sequences integrated into the mitochondrial genome of the chestnut blight fungus *Cryphonectria parasitica* (AAB84226.1 and CAA73185.1, exhibiting 63% similarity), with lesser similarity (<50%) observed in *Sclerotinia nivalis* and *Neurospora intermedia* mitogenomes, and in *Pleospora typhicola* plasmid.

Discrepancies in intron number and content are emphasized within the nad1, nad2, nad5, cob, cox2, and rns genes. As observed in the *A. bisporus* mitogenome [62], a majority of *A. subrufescens* mitochondrial group I introns harbor a homing endonuclease gene encoding a DNA endonuclease. The intron variation identified in both species implies a complex mechanism of intron loss and gain following species divergence and evolution.

Moreover, *A. subrufescens* mtDNA also harbors an additional and chimeric *nad2* gene copy. This chimeric gene has 1355 bp in length, in comparison to and 3302 bp found in both *A. subrufescens* and *A. bisporus* mitogenomes. However, only the region corresponding to the first 522 bp from the N-terminal of the protein coding sequence shows 75% of similarity. The rest of the predicted peptide, including the C-terminal, does not show any similarity with sequences available in public databases. Further transmembrane helices prediction based on the DeepTMHMM algorithm [74] revealed at least five transmembrane domains in the C-terminal, strongly suggesting that the protein product of this gene may be embedded in the membrane showing a predicted function similar to mitochondrial complex I and energy production.

Finally, while both mitogenomes carry the same set of 20 distinct tRNAs, minor variations in the location of each tRNA locus have been observed. For example, the *A. subrufescens* mtDNA displays a unique tRNA-Ile situated downstream of the *nad2* gene, and a tRNA-Thr positioned upstream of the *rns* gene. In contrast, the *A. bisporus* mtDNA exhibits a tRNA-Gly situated between the *atp8*

and *nad1* genes, as well as a duplicated cluster of tRNAs found in both inverted repeats.

4. Conclusion

In conclusion, we have successfully assembled the first high-quality chromosome-scale genome of *A. subrufescens*, the "sun mushroom," using a hybrid approach combining Illumina and Nanopore sequencing. This genome sequence provides valuable information about the genetic background of *A. subrufescens*, including the identification of PPO genes and the Mating-type locus. The genome assembly and annotation results are publicly available through a Genome Browser and can serve as a useful resource for further studies in fungal biology and genomics. The availability of the genome sequence may also lead to new cultivation alternatives or the application of gene editing strategies to delay the browning process and reduce post-harvest losses, which will increase the availability of this mushroom to consumers in various forms.

Data accessibility

The assembled genome sequence of *A. subrufescens* ABL 04/49 has been deposited with the NCBI under BioProject PRJNA926637 and accession number JAQOTE000000000. Raw genomic sequencing data were deposited in the SRA bank under accession numbers SRR23198184 (Illumina), and SRR23198183 (ONT). The predicted genes/proteins dataset is freely available for download from Zenodo at https://zenodo.org/record/8199855 (DOI: 10.5281/zenodo.8199855). A genome browser utilizing JBrowse2 [65], which contains our complete set of genomic data, is available at: https://plantgenomics.ncc.unesp.br/gen.php?id=Asub.

Declaration of competing interest

The authors declares that there is no conflict of interest.

Acknowledgements

We would like to thank the Minas Gerais Research Foundation (FAPEMIG) for providing financial support for this research project. CGA received a PhD scholarship from FAPEMIG, and AMV and VSP received a research fellowship from the Conselho Nacional de Desenvolvimento Científico e Tecnológico (CNPq) (#303061/2019−7 and #302569/2021-9, respectively). This research was supported by Coordenação de Aperfeiçoamento de Pessoal de Nível Superior — Brasil (CAPES) — Finance Code 001. In addition, we extend our gratitude to the Brazilian Microbiome Project (http://www.brmicrobiome.org) for their support in this study.

Appendix A. Supplementary data

Supplementary data to this article can be found online at https://doi.org/10.1016/j.resmic.2023.104116.

References

[1] da Eira AF, Didukh MY, de Amazonas MAL, Stamets P. Is a widely cultivated culinary-medicinal royal sun Agaricus (champignon do Brazil, or the himematsutake mushroom) Agaricus brasiliensis S.Wasser et al. Indeed a Synonym of A. subrufescens Peck? Int J Medicinal Mushrooms 2005;7(3):507−11. https://doi.org/10.1615/intjmedmushr.v7.i3.70.

[2] Herreira KMS, Alves E, Costa MD, Dias ES. Electron microscopy studies of basidiosporogenesis in Agaricus brasiliensis. Mycologia 2012;104(6):1272−80. https://doi.org/10.3852/11-294.

[3] Kerrigan RW. Agaricus subrufescens, a cultivated edible and medicinal mushroom, and its synonyms. Mycologia 2005;97(1):12−24. https://doi.org/10.3852/mycologia.97.1.12.

[4] Kerrigan RW. Inclusive and Exclusive Concepts of Agaricus subrufescens Peck: a Reply to Wasser et al. Int J Med Mushrooms 2007;9(1):79−84. https://doi.org/10.1615/intjmedmushr.v9.i1.100.

[5] Souza Dias E, Labory CRG, Herrera KMS, Alves AA, Torres GA, Rinker DL. Cytological studies of *Agaricus brasiliensis*. World J Microbiol Biotechnol 2008;24(11):2473−9. https://doi.org/10.1007/s11274-008-9769-4.

[6] Stamets P, Wasser SP, da Eira AF, Didukh MY, de Amazonas MAL. Is a widely cultivated culinary-medicinal royal sun Agaricus (the himematsutake mushroom) indeed *Agaricus blazei* Murrill. Int J Med Mushrooms 2002;4(4):24. https://doi.org/10.1615/intjmedmushr.v4.i4.10.

[7] Zied DC, Vieira Junior WG, Soares DMM, Stevani CV, Dias ES, Iossi MR, et al. Overview of four *Agaricus subrufescens* strains used in the last 15 years in Brazil and other countries and current potential materials for the future. Mycol Prog 2021;20(8):953−66. https://doi.org/10.1007/s11557-021-01711-x.

[8] Pardo-Giménez A, Pardo JE, Dias ES, Rinker DL, Caitano CEC, Zied DC. Optimization of cultivation techniques improves the agronomic behavior of Agaricus subrufescens. Sci Rep 2020;10(1):8154. https://doi.org/10.1038/s41598-020-65081-2.

[9] Sabino Ferrari AB, Azevedo de Oliveira G, Mannochio Russo H, Carvalho Bertozo L, Silva Bolzani V, Cunha Zied D, et al. *Pleurotus ostreatus* and *Agaricus subrufescens*: investigation of chemical composition and antioxidant properties of these mushrooms cultivated with different handmade and commercial supplements. Int J Food Sci Technol 2021;56(1):452−60. https://doi.org/10.1111/ijfs.14660.

[10] Smiderle FR, Ruthes AC, van Arkel J, Chanput W, Iacomini M, Wichers HJ, et al. Polysaccharides from *Agaricus bisporus* and *Agaricus brasiliensis* show similarities in their structures and their immunomodulatory effects on human monocytic THP-1 cells. BMC Compl Alternative Med 2011;11(58). https://doi.org/10.1186/1472-6882-11-58.

[11] Sorimachi K, Ikehara Y, Maezato G, Okubo A, Yamazaki S, Akimoto K, et al. Inhibition by *Agaricus blazei* Murill fractions of cytopathic effect induced by western equine encephalitis (WEE) virus on VERO cells in vitro. Biosci, Biotechnol, Biochem 2001;65(7):1645−7. https://doi.org/10.1271/bbb.65.1645.

[12] Ayeka PA. Potential of mushroom compounds as immunomodulators in cancer immunotherapy: a review. Evid base Compl Alternative Med: eCAM 2018;2018:7271509. https://doi.org/10.1155/2018/7271509.

[13] da Silva de Souza AC, Correa VG, Goncalves G, de A, Soares AA, Bracht A, et al. Agaricus blazei bioactive compounds and their effects on human health: benefits and controversies. Curr Pharmaceut Des 2017;23(19):2807−34. https://doi.org/10.2174/1381612823666170119093719.

[14] Gonzaga MLC, Bezerra DP, Alves APNN, de Alencar NMN, Mesquita R, de O, et al. In vivo growth-inhibition of Sarcoma 180 by an alpha-(1−>4)-glucan-beta-(1−>6)-glucan-protein complex polysaccharide obtained from *Agaricus blazei* Murill. J Nat Med 2009;63(1):32−40. https://doi.org/10.1007/s11418-008-0286-4.

[15] Levitz SM. Innate recognition of fungal cell walls. PLoS Pathogens 2010;6(4):e1000758. https://doi.org/10.1371/journal.ppat.1000758.

[16] Venkatesh Gobi V, Rajasankar S, Ramkumar M, Dhanalakshmi C, Manivasagam T, Justin Thenmozhi A, et al. *Agaricus blazei* extract attenuates rotenone-induced apoptosis through its mitochondrial protective and antioxidant properties in SH-SY5Y neuroblastoma cells. Nutr Neurosci 2018;21(2):97−107. https://doi.org/10.1080/1028415X.2016.1222332.

[17] Wisitrassameewong K, Karunarathna SC, Thongklang N, Zhao R, Callac P, Moukha S, et al. *Agaricus subrufescens*: a review. Saudi J Biol Sci 2012;19(2):131−46. https://doi.org/10.1016/j.sjbs.2012.01.003.

[18] Morin E, Kohler A, Baker AR, Foulongne-Oriol M, Lombard V, Nagy LG, et al. Genome sequence of the button mushroom *Agaricus bisporus* reveals mechanisms governing adaptation to a humic-rich ecological niche. 43. In: Proceedings of the National Academy of Sciences of the United States of America. 109; 2012. p. 17501−6. https://doi.org/10.1073/pnas.1206847109.

[19] do Valle JS, Vandenberghe LP de S, Santana TT, Linde GA, Colauto NB, Soccol CR. Optimization of Agaricus blazei laccase production by submerged cultivation with sugarcane molasses. Afr J Microbiol Res 2014;8(9):939−46. https://doi.org/10.5897/ajmr2013.6508.

[20] Royse DJ, Baars J, Tan Q. Current overview of mushroom production in the world. In Edible and Medicinal Mushrooms. John Wiley & Sons, Ltd 2017:5−13. https://doi.org/10.1002/9781119149446.ch2.

[21] Joshi K, Warby J, Valverde J, Tiwari B, Cullen PJ, Frias JM. Impact of cold chain and product variability on quality attributes of modified atmosphere packed mushrooms (*Agaricus bisporus*) throughout distribution. J Food Eng 2018;232:44−55. https://doi.org/10.1016/j.jfoodeng.2018.03.019.

[22] Lei J, Li B, Zhang N, Yan R, Guan W, Brennan CS, et al. Effects of UV-C treatment on browning and the expression of polyphenol oxidase (PPO) genes in different tissues of *Agaricus bisporus* during cold storage. Postharvest Biol Technol 2018;139:99−105. https://doi.org/10.1016/j.postharvbio.2017.11.022.

[23] Lin X, Sun D-W. Research advances in browning of button mushroom (*Agaricus bisporus*): affecting factors and controlling methods. Trends Food Sci Technol 2019;90:63−75. https://doi.org/10.1016/j.tifs.2019.05.007.

[24] Brandenburger E, Braga D, Kombrink A, Lackner G, Gressler J, Künzler M, et al. Multi-genome analysis identifies functional and phylogenetic diversity of

basidiomycete adenylate-forming reductases. Fungal Genet Biol: FG & B 2018;112:55–63. https://doi.org/10.1016/j.fgb.2016.07.008.
[25] Ohm RA, de Jong JF, Lugones LG, Aerts A, Kothe E, Stajich JE, et al. Genome sequence of the model mushroom *Schizophyllum commune*. Nat Biotechnol 2010;28(9):957–63. https://doi.org/10.1038/nbt.1643.
[26] Chen S, Xu J, Liu C, Zhu Y, Nelson DR, Zhou S, et al. Genome sequence of the model medicinal mushroom Ganoderma lucidum. Nat Commun 2012;3:913. https://doi.org/10.1038/ncomms1923.
[27] Bao D, Gong M, Zheng H, Chen M, Zhang L, Wang H, et al. Sequencing and comparative analysis of the straw mushroom (Volvariella volvacea) genome. PloS One 2013;8(3):e58294. https://doi.org/10.1371/journal.pone.0058294.
[28] Park Y-J, Baek JH, Lee S, Kim C, Rhee H, Kim H, et al. Whole genome and global gene expression analyses of the model mushroom *Flammulina velutipes* reveal a high capacity for lignocellulose degradation. PloS One 2014;9(4):e93560. https://doi.org/10.1371/journal.pone.0093560.
[29] Chen L, Gong Y, Cai Y, Liu W, Zhou Y, Xiao Y, et al. Genome sequence of the edible cultivated mushroom Lentinula edodes (Shiitake) reveals insights into lignocellulose degradation. PloS One 2016;11(8):e0160336. https://doi.org/10.1371/journal.pone.0160336.
[30] Kiyama R, Furutani Y, Kawaguchi K, Nakanishi T. Genome sequence of the cauliflower mushroom *Sparassis crispa* (Hanabiratake) and its association with beneficial usage. Sci Rep 2018;8(1):16053. https://doi.org/10.1038/s41598-018-34415-6.
[31] Yuan Y, Wu F, Si J, Zhao Y-F, Dai Y-C. Whole genome sequence of *Auricularia heimuer* (Basidiomycota, Fungi), the third most important cultivated mushroom worldwide. Genomics 2019;111(1):50–8. https://doi.org/10.1016/j.ygeno.2017.12.013.
[32] Gong W, Wang Y, Xie C, Zhou Y, Zhu Z, Peng Y. Whole genome sequence of an edible and medicinal mushroom, *Hericium erinaceus* (Basidiomycota, Fungi). Genomics 2020;112(3):2393–9. https://doi.org/10.1016/j.ygeno.2020.01.011.
[33] Yu F, Song J, Liang J, Wang S, Lu J. Whole genome sequencing and genome annotation of the wild edible mushroom, russula griseocarnosa. Genomics 2020;112(1):603–14. https://doi.org/10.1016/j.ygeno.2019.04.012.
[34] Lee Y-Y, Vidal-Diez de Ulzurrun G, Schwarz EM, Stajich JE, Hsueh Y-P. Genome sequence of the oyster mushroom *Pleurotus ostreatus* strain PC9. G3-GENES GENOM GENET 2021;11(2). https://doi.org/10.1093/g3journal/jkaa008.
[35] Wan J-N, Li Y, Guo T, Ji G-Y, Luo S-Z, Ji K-P, et al. Whole-genome and transcriptome sequencing of reveals its associated ectomycorrhizal niche and conserved pathways involved in fruiting body development. Front Microbiol 2021;12:732458. https://doi.org/10.3389/fmicb.2021.732458.
[36] Sonnenberg ASM, Sedaghat-Telgerd N, Lavrijssen B, Ohm RA, Hendrickx PM, Scholtmeijer K, et al. Telomere-to-telomere assembled and centromere annotated genomes of the two main subspecies of the button mushroom *Agaricus bisporus* reveal especially polymorphic chromosome ends. Sci Rep 2020;10(1):14653. https://doi.org/10.1038/s41598-020-71043-5.
[37] Zied DC, Pardo Gimenez A, Pardo Gonzalez JE, Souza Dias E, Carvalho MA, Minhoni MTDA. Effect of cultivation practices on the β-glucan content of Agaricus subrufescens basidiocarps. J Agric Food Chem 2014;62(1):41–9.
[38] Vieira Junior WG, Centeio Cardoso RV, Fernandes Â, Ferreira ICFR, Barros L, Pardo-Giménez A, et al. Influence of strains and environmental cultivation conditions on the bioconversion of ergosterol and vitamin D2 in the sun mushroom. J Sci Food Agric 2022;102(4):1699–706.
[39] de Lima Ferreira JK, de Mello Varani A, Tótola MR, Fernandes Almeida M, de Sousa Melo D, Ferreira Silva E Batista C, et al. Phylogenomic characterization and pangenomic insights into the surfactin-producing bacteria Bacillus subtilis strain RI4914 [publication of the Brazilian Society for Microbiology] Braz J Microbiol 2022;53(4):2051–63. https://doi.org/10.1007/s42770-022-00815-0.
[40] Marçais G, Kingsford C. A fast, lock-free approach for efficient parallel counting of occurrences of k-mers. Bioinformatics 2011;27(6):764–70. https://doi.org/10.1093/bioinformatics/btr011.
[41] Vurture GW, Sedlazeck FJ, Nattestad M, Underwood CJ, Fang H, Gurtowski J, et al. GenomeScope: fast reference-free genome profiling from short reads. Bioinformatics 2017;33(14):2202–4. https://doi.org/10.1093/bioinformatics/btx153.
[42] Zimin AV, Marçais G, Puiu D, Roberts M, Salzberg SL, Yorke JA. The MaSuRCA genome assembler. Bioinformatics 2013;29(21):2669–77. https://doi.org/10.1093/bioinformatics/btt476.
[43] Alonge M, Lebeigle L, Kirsche M, Jenike K, Ou S, Aganezov S, et al. Automated assembly scaffolding using RagTag elevates a new tomato system for high-throughput genome editing. Genome Biol 2022;23(1):258. https://doi.org/10.1186/s13059-022-02823-7.
[44] Li H. Minimap2: pairwise alignment for nucleotide sequences. Bioinformatics 2018;34(18):3094–100. https://doi.org/10.1093/bioinformatics/bty191.
[45] Foulongne-Oriol M, Rocha de Brito M, Cabannes D, Clément A, Spataro C, Moinard M, et al. The genetic linkage map of the medicinal mushroom Agaricus subrufescens reveals highly conserved macrosynteny with the congeneric species agaricus bisporus. G3-GENES GENOM GENET 2016;6(5):1217–26. https://doi.org/10.1534/g3.115.025718.
[46] Kim J, Park M-J, Shim D, Ryoo R. De novo genome assembly of the bioluminescent mushroom *Omphalotus guepiniiformis* reveals an Omphalotus-specific lineage of the luciferase gene block. Genomics 2022;114(6):110514. https://doi.org/10.1016/j.ygeno.2022.110514.
[47] Chor B, Horn D, Goldman N, Levy Y, Massingham T. Genomic DNA k-mer spectra: models and modalities. Genome Biol 2009;10(10):R108. https://doi.org/10.1186/gb-2009-10-10-r108.
[48] Rhie A, Walenz BP, Koren S, Phillippy AM. Merqury: reference-free quality, completeness, and phasing assessment for genome assemblies. Genome Biol 2020;21(1):245. https://doi.org/10.1186/s13059-020-02134-9.
[49] Ou S, Su W, Liao Y, Chougule K, Agda JRA, Hellinga AJ, et al. Benchmarking transposable element annotation methods for creation of a streamlined, comprehensive pipeline. Genome Biol 2019;20(1):275. https://doi.org/10.1186/s13059-019-1905-y.
[50] Grabherr MG, Haas BJ, Yassour M, Levin JZ, Thompson DA, Amit I, et al. Full-length transcriptome assembly from RNA-Seq data without a reference genome. Nat Biotechnol 2011;29(7):644–52. https://doi.org/10.1038/nbt.1883.
[51] Haas BJ, Salzberg SL, Zhu W, Pertea M, Allen JE, Orvis J, et al. Automated eukaryotic gene structure annotation using EVidenceModeler and the Program to Assemble Spliced Alignments. Genome Biol 2008;9(1):R7. https://doi.org/10.1186/gb-2008-9-1-r7.
[52] Hoff KJ, Lomsadze A, Borodovsky M, Stanke M. Whole-genome annotation with BRAKER. Methods Mol Biol 2019;1962:65–95. https://doi.org/10.1007/978-1-4939-9173-0_5.
[53] Kuznetsov D, Tegenfeldt F, Manni M, Seppey M, Berkeley M, Kriventseva EV, et al. OrthoDB v11: annotation of orthologs in the widest sampling of organismal diversity. Nucleic Acids Res 2023;51(D1):D445–51. https://doi.org/10.1093/nar/gkac998.
[54] Huerta-Cepas J, Szklarczyk D, Heller D, Hernández-Plaza A, Forslund SK, Cook H, et al. eggNOG 5.0: a hierarchical, functionally and phylogenetically annotated orthology resource based on 5090 organisms and 2502 viruses. Nucleic Acids Res 2019;47(D1):D309–14. https://doi.org/10.1093/nar/gky1085.
[55] Coudert E, Gehant S, de Castro E, Pozzato M, Baratin D, Neto T, et al. UniProt consortium. Annotation of biologically relevant ligands in UniProtKB using ChEBI Bioinformatics 2023;39(1). https://doi.org/10.1093/bioinformatics/btac793.
[56] Conesa A, Götz S, García-Gómez JM, Terol J, Talón M, Robles M. Blast2GO: a universal tool for annotation, visualization and analysis in functional genomics research. Bioinformatics 2005;21(18):3674–6. https://doi.org/10.1093/bioinformatics/bti610.
[57] Kanehisa M, Sato Y, Morishima K. BlastKOALA and GhostKOALA: KEGG tools for functional characterization of genome and metagenome sequences. J Mol Biol 2016;428(4):726–31. https://doi.org/10.1016/j.jmb.2015.11.006.
[58] Blin K, Shaw S, Kloosterman AM, Charlop-Powers Z, van Wezel GP, Medema MH, et al. antiSMASH 6.0: improving cluster detection and comparison capabilities. Nucleic Acids Res 2021;49(W1):W29–35. https://doi.org/10.1093/nar/gkab335.
[59] Yin Y, Mao X, Yang J, Chen X, Mao F, Xu Y. dbCAN: a web resource for automated carbohydrate-active enzyme annotation. Nucleic Acids Res 2012;40:W445–51. https://doi.org/10.1093/nar/gks479.
[60] Zhang H, Yohe T, Huang L, Entwistle S, Wu P, Yang Z, et al. dbCAN2: a meta server for automated carbohydrate-active enzyme annotation. Nucleic Acids Res 2018;46(W1):W95–101. https://doi.org/10.1093/nar/gky418.
[61] Xu L, Dong Z, Fang L, Luo Y, Wei Z, Guo H, et al. OrthoVenn2: a web server for whole-genome comparison and annotation of orthologous clusters across multiple species. Nucleic Acids Res 2019;47(W1):W52–8. https://doi.org/10.1093/nar/gkz333.
[62] Férandon C, Xu J, Barroso G. The 135 kbp mitochondrial genome of *Agaricus bisporus* is the largest known eukaryotic reservoir of group I introns and plasmid-related sequences. Fungal Genet Biol: FG & B 2013;55:85–91. https://doi.org/10.1016/j.fgb.2013.01.009.
[63] Gilchrist CLM, Chooi Y-H. Clinker & clustermap.js: automatic generation of gene cluster comparison figures. Bioinformatics 2021;37(16):2473–5. https://doi.org/10.1093/bioinformatics/btab007.
[64] Wintersinger JA, Wasmuth JD. Kablammo: an interactive, web-based BLAST results visualizer. Bioinformatics 2015;31(8):1305–6. https://doi.org/10.1093/bioinformatics/btu808.
[65] Diesh C, Stevens GJ, Xie P, De Jesus Martinez T, Hershberg EA, Leung A, et al. JBrowse 2: a modular genome browser with views of synteny and structural variation. Genome Biol 2023;24(1):74. https://doi.org/10.1186/s13059-023-02914-z. Apr 17.
[66] Li H, Wu S, Ma X, Chen W, Zhang J, Duan S, et al. The genome sequences of 90 mushrooms. Scientific Reports 2018;8(1):9982. https://doi.org/10.1038/s41598-018-28303-2.
[67] Mohanta TK, Bae H. The diversity of fungal genome. Biol Proced Online 2015;17(8). https://doi.org/10.1186/s12575-015-0020-z.
[68] O'Connor E, McGowan J, McCarthy CGP, Amini A, Grogan H, Fitzpatrick DA. Whole genome sequence of the commercially relevant mushroom strain var. ARP23. G3-GENES GENOM GENET 2019;9(10):3057–66. https://doi.org/10.1534/g3.119.400563.
[69] Floudas D, Binder M, Riley R, Barry K, Blanchette RA, Henrissat B, et al. The Paleozoic origin of enzymatic lignin decomposition reconstructed from 31 fungal genomes. Science 2012;336(6089):1715–9. https://doi.org/10.1126/science.1221748.
[70] Kidwai M, Ahmad IZ, Chakrabarty D. Class III peroxidase: an indispensable enzyme for biotic/abiotic stress tolerance and a potent candidate for crop

improvement. Plant Cell Rep 2020;39(11):1381–93. https://doi.org/10.1007/s00299-020-02588-y.
[71] Foulongne-Oriol M, Taskent O, Kües U, Sonnenberg ASM, van Peer AF, Giraud T. Mating-type locus organization and mating-type chromosome differentiation in the bipolar edible button mushroom. Genes 2021;12(7). https://doi.org/10.3390/genes12071079.
[72] Kang X, Hu L, Shen P, Li R, Liu D. SMRT sequencing revealed mitogenome characteristics and mitogenome-wide DNA modification pattern in. Front Microbiol 2017;8:1422. https://doi.org/10.3389/fmicb.2017.01422.
[73] Yuan X, Feng C, Zhang Z, Zhang C. Complete mitochondrial genome of and identification of molecular markers for the oomycetes. Front Microbiol 2017;8:1484. https://doi.org/10.3389/fmicb.2017.01484.
[74] Hallgren J, Tsirigos KD, Pedersen MD, Almagro Armenteros JJ, Marcatili P, Nielsen H, et al. DeepTMHMM predicts alpha and beta transmembrane proteins using deep neural networks. In bioRxiv 2022. https://doi.org/10.1101/2022.04.08.487609.